Secondary metabolites of the leaves of *Tricalysia atherura* N. Hallé (Rubiaceae) and their potential antiplasmodial activity

Gwladys Djikam Sime [a,e], Mbabi Nyemeck II Norbert [a,c], Auguste Abouem A Zintchem [a,b], Natasha October[d], Marius Balemaken Missi [a,d], Rabia Farooq[e], Khalid Mohammed Khan[e], Dominique Serge Ngono Bikobo [a*], Muhammad Iqbal Choudhary[e], Dieudonné Emmanuel Pegnyemb[a]

[a] Faculty of science, Department of Organic Chemistry, University of Yaoundé 1, Yaoundé, Cameroon

[b] Department of Chemistry, Higher Teacher's Training College, University of Yaoundé 1, P.O. Box 47, Yaoundé, Cameroon;

[c] Department of Chemistry, Faculty of Science, University of Dschang, P.O. Box 67, Dschang, Cameroon;

[d] Department of Chemistry, University of Pretoria, Hatfield 0028, South Africa;

[e] International Center for Chemical and Biological Sciences, H.E.J Research Institute of Chemistry, University of Karachi, Karachi-75270, Pakistan

*CONTACT: Dominique Serge Ngono Bikobo. Email: ngono_serge@yahoo.fr

Graphical Abstract

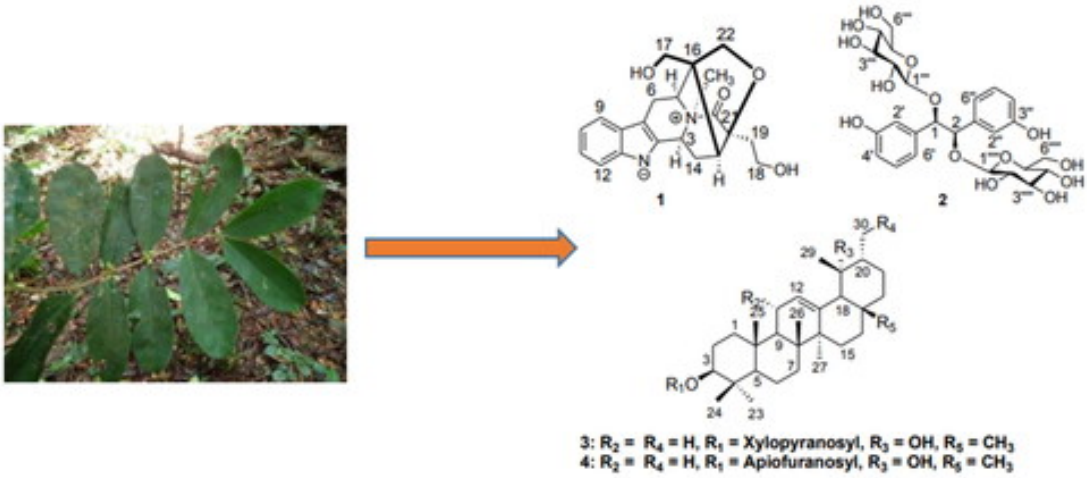

Abstract

One monoterpene indole alkaloid, atheruramine (**1**) bearing an ether bridge linking, one hydrobenzoin derivative, tricalydioloside (**2**) and two ursane-type triterpenes, atherurosides (A and B) (**3** and **4**) were isolated from the leaves of *Tricalysia atherura*, together with eight known compounds. The structures of these new compounds were elucidated on the basis of the results of spectroscopic analysis, and the relative configurations of compounds **1–3** were established by NOE difference. Four of the metabolites were screened *in vitro* against both chloroquine (CQ)-sensitive (3D7) and -resistant (Dd2) strains of *Plasmodium falciparum*; they were found to exhibit moderate activity against chloroquine-resistant (Dd2) (IC_{50} 64.99–92.29 µg/mL). Meanwhile, crude extract possesses high antiplasmodial activity against both 3D7 and Dd2 strains of *P. falciparum* (IC_{50} 4.39–7.54 µg/mL) and high selectivity indices values (SI > 10) and was found to be safe.

Keywords: *Tricalysia atherura*; Rubiaceae; indole alkaloid; atheruramine; hydrobenzoin derivative; pentacyclic triterpenes; antiplasmodial; cytotoxic activities

1. Introduction

Malaria is one of the major public health challenges undermining development in the poorest countries, especially in Sub-Saharan Africa. According to the latest 'World malaria report', in 2019, there were 229 million cases of malaria in 87 endemic countries, with 94% of cases mainly in African Region. Each year, more than 400 thousand people die of malaria. An estimated two thirds of deaths are among children under the age of five (WHO 2020). Recently, WHO recommended widespread use of the RTS,S/AS01 (RTS,S) vaccine (Mosquirix^{TM}) among children in Sub-Saharan Africa and in the regions with moderate to high *P. falciparum* malaria transmission (Laurens 2020; WHO 2021). Indeed, the impact of this vaccine will be the relative significant reduction (30%) in deadly severe malaria and the highly cost-effective of this vaccine. Currently, in Sub-Saharan Africa, only 40% of inhabitants can access public health system (WHO 2004) and most of them still rely on traditional medicine for most of their health care needs. Medicinal plants are biologically and chemically diverse resource as they synthesize various chemicals as defence agents against pests, diseases and predators. They are an excellent reservoir of medicines and chemical leads from which researchers can design and synthesize new drugs. In fact, about 25% of the drugs used in modern medicine owe their origins to plants from tropical rainforest (Elliot 1986). In this context, Rubiaceae family is characterized by the production of bioactive metabolites with great pharmacological potential (Barreiro 1990; Farias 2006). It is a cosmopolitan distribution family, mostly focused in the tropics. Being one of the largest in the *Magnoliopsidae* class, it ranks fourth in diversity of species among Angiosperms (Mabberley 1990). It includes approximately 637 genera and 13,000 species (Mongrand et al. 2005; Pereira and Meireles 2010). *Tricalysia* is an important genus of Rubiaceae family, largely confined to rainforest and especially in Guineo-Congolian Region of Africa and it consists of 79 to 96 species (Bridson and Verdcourt 2003). *Tricalysia atherura* is a relatively rare species, which is a shrub up to 10 m tall with young twigs puberulous with elliptical and lanceolate leaves and ribbed fruits (Sonké et al. 2002). It is found generally in tropical regions of Africa and usually at higher altitude in Cameroon such as the Korup National Park in the southwest Region of Cameroon (Robbrecht 1987; Sonké et al. 2002). Due to the lack of comprehensive report on the ethnomedicinal uses of *Tricalysia atherura*, several species of the genus *Tricalysia* have widespread been used in folk medicine

to treat various ailments such as: stomachache, constipation, earache, malaria, jaundice, severe fevers, joint pain and skin diseases (Bouquet 1972; Bruschi et al. 2011; Moshi et al. 2012). Also, few are used as sedative and emetic (Moshi et al. 2012). To our knowledge, there is no scientific report on antimalarial activity of either *T. atherura* or any of its constituents. However, its genus presents a large diversity of compounds such as: iridoids, indole alkaloids, anthraquinones, cerebrosides, terpenoids (diterpenes and triterpenes), flavonoids, steroids and other phenolic derivatives (He et al. 2002; Nishimura et al. 2006; Xu et al. 2010; Awouafack et al. 2018). In the course of our continuous interest in identifying new potential antimalarials from Cameroonian flora, the chemical constituents of the EtOAc-soluble fraction of the 80% MeOH extract of the leaves of *T. atherura* have been investigated. As a result, a total of 12 compounds were isolated and characterized, including four undescribed ones among which, one indole alkaloid (**1**), one glycosylated stilbene derivative (**2**) and two ursane type-triterpenes (**3** and **4**). Reported herein are their isolation, structure determination, and their antiplasmodial activities against two strains of *Plasmodium falciparum* 3D7 and Dd2.

2. Results and discussion

The 80% MeOH extract of the leaves of *T. atherura* (3.5 kg, air-dried) was suspended in H_2O and then partitioned successively with n-hexane, EtOAc, and n-BuOH respectively. The entire EtOAc-soluble fraction was subjected repeatedly to column chromatography (CC) over silica gel, Sephadex LH-20, and semi-preparative HPLC to afford twelve compounds (**1–12**). In addition to the new isolates (**1**–**4**), eight known compounds were isolated and identified as: 19α-hydroxy-amyrin (**5**) (Akbar and Malik 2002), uvaol (**6**) (Greve et al. 2017), ursolic acid (**7**) (Akbar and Malik 2002), rubrinol (**8**) (Akhtar et al. 1994), strictosidinic acid (**9**) (De Silva et al. 1971), tricalysiolide B (10) (Nishimura et al. 2006), tricalysiamide B (**11**) (Nishimura et al. 2007) and asarinin (**12**) (Parmar et al. 1998), by comparison of their spectroscopic data and physicochemical properties (Figure 1).

Compound **1** was obtained as an optically active white amorphous solid, $[\alpha_D^{25}]$ – 43.7 (*c* 1.0, MeOH). The IR spectrum showed two important absorptions at 3385 and 1678 cm^{-1} for hydroxyl and carbonyl groups, respectively, while the UV absorption bands at λ_{max} 225 and 290 nm indicated an indole chromophore (Brown and Charalambides 1974). Its molecular formula $C_{21}H_{24}N_2O_4$, was established by HR-ESI-MS at *m/z* 369.1805 $[M + H]^+$(calcd. for $C_{21}H_{25}N_2O_4^+$: 369.1809).

Analysis of the ^1H NMR data (Table S1) suggested the presence of four aromatic hydrogens, corresponding to an unsubstituted indole ring at δ_H 6.96 (1H, dd, *J* = 8.0; 7.8 Hz, H–10), 7.04 (1H, dd, *J* = 8.0; 7.6 Hz, H–11), 7.27 (1H, d, *J* = 8.5 Hz, H–12) and 7.36 (1H, d, *J* = 8.0 Hz, H–9), one *N*-methyl at δ_H 3.07, and three pair of oxymethylene protons at δ_H 2.88 (2H, brs, H–17), 3.67 (1H, d, *J* = 14.0 Hz, H–22β)/3.75 (1H, overl, H–22α), and 3.76 (2H, overl, H–18). The ^{13}C NMR and DEPT spectra revealed 21 resonances, comprising 4 sp^2 quarternary carbons, 4 sp^2 methines, 1 *N*-methyl, 3 sp^3 methylenes, 3 sp^3 methines, 2 sp^3 quarternary carbons, 3 sp^3 oxymethylenes, one amide carbonyl group (Figures S7, S8). The above data revealed that the structure of **1** was similar to that of *N*-methylakuammidine (Nogueira et al. 2014). Both differ by the presence of a hydroxyethyl fragment at C–20 and an oxymethylene attached to C–22 in **1** instead of the double bond between C–18 and C–19, the carboxyle group at C–22, respectively in *N*-methylakuammidine. The COSY and HSQC supported the presence of an unsubstituted indole moiety and *N*-methyl group, an isolated hydroxymethylene, one $-CH_2O-$ unit, and a hydroxyethyl fragment. This was further confirmed by the HMBC cross-peaks of H–5 and H–15 (δ_H 3.40 and δ_H 2.22 respectively) to C–21 (Figures S10, S11)

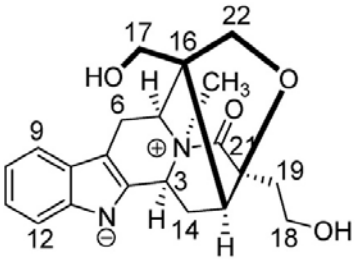

1: Atherumamine

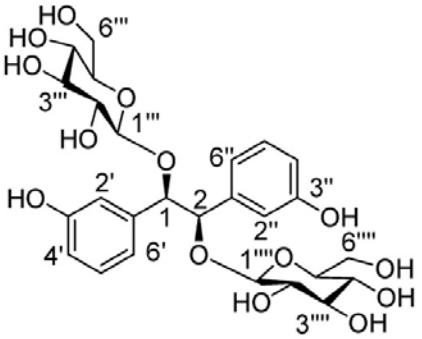

2: Tricalydioloside

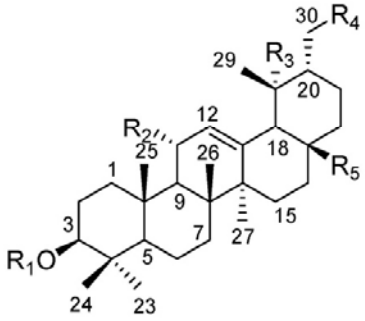

3: R_2 = R_4 = H, R_1 = Xylopyranosyl, R_3 = OH, R_5 = CH_3; **Atherioside A**
4: R_2 = R_4 = H, R_1 = Apiofuranosyl, R_3 = OH, R_5 = CH_3; **Atherioside B**
5: R_1 = R_2 = R_4 = H, R_3 = OH, R_5 = CH_3; **19α-hydroxy-amyrin**
6: R_1 = R_3 = R_4 = H, R_2 = OCH_3, R_5 = CH_3; **Uvaol**
7: R_1 = R_3 = R_4 = R_2 = H, R_5 = COOH; **Ursolic acid**
8: R_1 = R_2 = R_3 = R_5 = H, R_4 = OH; **Rubrinol**

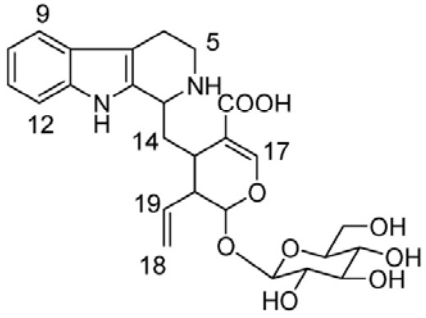

9: strictosidinic acid

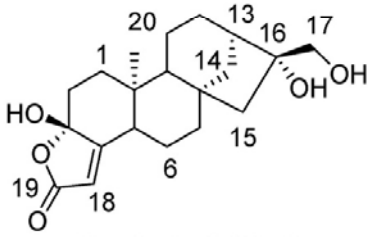

10: tricalysiolide B

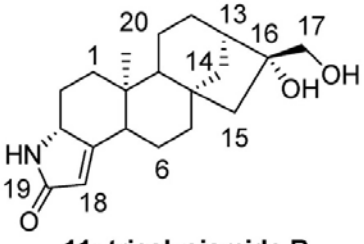

11: tricalysiamide B

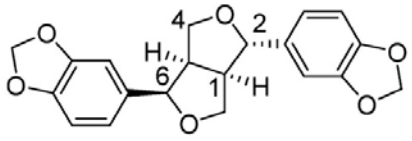

12: (+)-asarinin

Figure 1. Structures of compounds **1**–**12.**

providing additional support for the presence of a carbonyl function at C–21. Furthermore, the HMBC correlations of methyl signals at δ_H 3.09 to C–16 (δ_C 53.9) and C–5 (δ_C 61.2), and H–3 (δ_H 4.04) to C–15, C–5, C–14 revealed the presence of a *N*-methyl group in **1**. Moreover, an hexacyclic skeleton which includes one bridge between C–20 and C–22 was confirmed by an HMBC cross-peak from H–22*α*/22*β* (δ_H 3.67 and 3.75) to C–20 (δ_C 84.1), C–16 (δ_C 53.9) and C–15, and H–15 (δ_H 2.22) to C–20 and C–19 (δ_C 38.1) (Figure S12). The –CH_2CH_2OH unit was supported by the HMBC correlations from the isolated methylene hydrogens H–19*α*/*β* (δ_H 1.82/1.98) to C–20 (δ_C 84.1), C–15 (δ_C 38.6) and C–18 (δ_C 58.3) suggesting attachment of the hydroxylethyl side chain to the quaternary C–20 carbon, which was linked to an oxygen atom as was evident from its observed shift at δ_C 84.1. Insertion of an ether bridge linking the quaternary C–20 and the oxymethylene C–22, placement of an OH substituent at C–18 of a terminal vinyl group (double bond between C–18 and C–19 in **1** instead of the double bond between C–19 and C–20 for most common alkaloids), resulted to an isolated hydroxyethyl fragment with a complete assembly of the ring system of **1**, which is also in agreement with the full HMBC data (Figure S12). Additionally, the chemical shifts at C–3 (δ_C 49.2) and the *N*-methyl group (δ_C 51.6) in **1**, were very closed to those reported for *cis*-*N*-methylquinolizidinium moieties with chemical shifts at δ_C 49.6 and 48.9 (Bartlett et al. 1962; Kiang et al. 1966). Based on the above analysis, compound **1** was deduced as a zwitterion, supported by the significant upfield-shifted carbon atoms (C–3 and C–5: δ_C 49.2 and 61.2) neighboring the nitrogenated charges of **1** compared to those of *N*-methylakuammidine (C–3 and C–5; δ_C 60.7 and 66.3, downfield-shifted due to attractive effects of the positive nitrogen N_4) (Nogueira et al. 2014; Bitombo et al. 2021). The relative configuration of **1** was elucidated by Nuclear Overhauser Effect Spectroscopy (NOESY) correlations similar to that of the related sarpagine polycyclic framework in various natural derivatives (Battersby and Yeowell 1964; Puteri et al. 2019), especially macusine C (Battersby and Yeowell 1964). First, H–3 and H–5/N_4–CH_3 were assigned to be *α*-axially oriented from the NOESY correlations between H–3 and H–5/N_4–CH_3 while CH_2–17 were deduced to possess *β*-orientation from the NOESY correlations of H–17 with H–14*β*. Furthermore, the *α* configuration of H–15 and the hydroxyl ethyl group were confirmed by the NOE correlation of H–15 to H–19*α* and H–14*α* (Figures S2, S13). Therefore, the structure of atheruramine was elucidated as shown in Figure 1.

Compound **2** was obtained as an optically active amorphous yellow solid, $[\alpha_D^{25}]$ – 39.7 (*c* 1.0, MeOH). The IR spectrum, showed the absorption bands at 3380 (O–H stretching), 2920 (C–H stretching), 1562 (C–H bending for aromatic), 1455 (C–H bending), 1205 and 1032 cm^{-1} (C–O stretching). The UV absorption bands at λ_{max} = 226, 251 and 260 nm indicated a benzoin chromophore (Lim et al. 2021). Its molecular formula $C_{26}H_{34}O_{14}$, was established by HR-ESI-MS at *m*/*z* 571.2086 $[M + H]^+$(calcd. for $C_{26}H_{35}O_{14}^+$: 571.2084). The analysis of ^{1}H NMR spectrum (Table S2) suggested the presence of eight aromatic hydrogens corresponding to two disubstituted benzene ring systems at δ_H 6.85 (1H, overl, H–4′)/6.83 (1H, overl, H–4″), 6.99 (2H, overl, H–2′/H–2″), 7.02 (2H, overl, H–6′/H–6″) and 7.25 (1H, dd, *J* = 8.0; 7.5 Hz, H–5″)/7.24 (1H, dd, *J* = 8.0; 7.5 Hz, H–5′); two methine protons at δ_H 5.95 (1H, brs, H–1) and 5.81 (1H, brd, *J* = 1.0 Hz, H–2), which suggesting the presence of oxymethine groups, were supported by ^{13}C-NMR resonances occurring at δ_C 68.4 and 68.2 respectively. In addition, the ^{1}H-NMR spectrum of **2** also showed signals of two anomeric protons at δ_H 4.64 and 4.23 (1H each, d, *J* = 7.5 Hz, H–1‴ and H–1⁗ respectively). The protons of each monosaccharide residue were assigned starting from the readily identifiable anomeric protons using ^{1}H-^{1}H COSY and HSQC spectra. The ^{13}C NMR data and HSQC spectrum revealed 23 resonances, comprising 3 sp^2 quarternary carbons, 6 sp^2 methines, 2 sp^3 methylenes and 12 sp^3 methines (Figure S16). According to literature, the NMR data of **2** (Table S2) were similar to those of hydrobenzoin (Lim et al. 2021), differing mainly by the presence of quaternary phenolic carbon

atom at δ_C 159.3 (C–3′/3″) and two anomeric carbon atoms at δ_C 102.0 and 101.8 (C–1‴ and 1⁗), respectively in **2**. The ^{1}H–^{1}H COSY spectrum indicated that the oxygen–substituted methine proton at δ_H 5.95 (H–1) coupled with the second one at δ_H 5.81 (H–2). There were also correlations between all the aromatic protons in the ^{1}H-^{1}H COSY spectrum. The whole structure of this compound consists of three quaternary carbons; δ_C 159.3, 136.3 and 136.0 (C–3′/3″, C–1′ and C–1″ respectively), two different secondary carbons at δ_C 68.4 and 68.2 (C–1 and C–2) and distinguishable carbons of the glucopyranosyl moieties (δ_C 102.0, 78.3, 78.0, 74.6, 71.4 and 64.4 for the first sugar unit/δ_C 101.8, 78.3, 78.1, 73.8, 71.3 and 62.8 for the second sugar unit). The HMBC spectrum showed that the oxygen-substituted methine proton H–1 (δ_H 5.95) correlated with an oxygen substituted methine carbon C–2 (δ_C 68.2), and with aromatic carbons C–1′, C–2′ and C–6′. There were other correlations observed from the second oxygen-substituted methine H–2 (δ_H 5.81) with C–1 (δ_C 68.4) and aromatic carbons C–1″ and C–6″ (Figure S20). Furthermore, the HMBC correlations of anomeric proton signals H–1‴ at δ_H 4.64 to C–1 (δ_C 68.4) and H–1⁗ at δ_H 4.23 to C–2 (δ_C 68.2) indicated the connections of these sugars with vicinal hydroxy carbons C–1 and C–2 respectively. The aromatic protons at δ_H 6.99 were assigned as H–2′/2″, because they showed connectivities with C–1, C–1′, C–1″, C–2, C–3′ and C–3″ suggesting their attachment to the vicinal ethane diol side chain through quaternary C–1′ and C–1″ carbons. These analyses further supported the structure of 1,2-*O*,*O*-di-(*β*-D-glucopyranosyl)-1,2-bis(3-hydroxyphenyl)ethane for **2**. The relative configuration of C–2 could not be assigned by NOESY because there was no NOESY correlation between H–1 and H–2. However, it was deduced by comparison with the coupling constants and optical rotation data of similar compounds. The small characteristic coupling constant of H–1 and H–2 (J = 1.0 Hz), enabled a *trans*-relationship between both protons (Agata et al. 1988; Figure 1). Additionally, a comparison with literature data of related acyclic vicinal diol derivatives ((7'*R*, 8'*R*)-*threo*-streblusligna nol-2-*O*-*β*-D-glucopyranoside and 1-(4′-methoxyphenyl)-l,2-propanediol) (Li et al. 2012a; 2012b) led to the conclusion that the optical rotation, $[\alpha]_D$ can be assumed to the (*R*, *R*) configuration. Based on the above analysis, compound **2** was determined to be (1*R**, 2*R**)-*threo*-1,2-*O*,*O*-di-(*β*-D-glucopyranosyl)-1,2-bis(3-hydroxyphenyl)ethane, to which the trivial name tricalydioloside was given.

Compound **3** was obtained as white amorphous powder. It gave a positive Liebermann-Burchard's reaction (Gołembiewska et al. 2013), indicating its triterpenoidal nature. Its molecular formula was determined as $C_{35}H_{58}O_6$ based on the HR-ESI-MS *pseudo*-molecular ion peak at *m/z* 575.4068 $[M + H]^+$ (calcd. for $C_{35}H_{59}O_6^+$: 575.4075), requiring seven degrees of unsaturation. These degrees of unsaturation can be accounted for five rings system, one olefinic double bond and one monosaccharide group. Its IR absorption bands at 3448, 1619, 1205 and 1110 cm^{-1} suggested the presence of hydroxyl groups, double bond, C-*O*-C and C-OH bonds respectively. The ^{1}H NMR spectrum of **3** (Table S3) exhibited seven singlet methyls at δ_H 0.84 (3H, s, H–23), 1.03 (3H, s, H–24), 0.94 (3H, s, H–25), 0.76 (3H, s, H–26), 1.31 (3H, s, H–27), 0.92 (3H, s, H–28) and 1.18 (3H, s, H–29), and one doublet methyl group at δ_H 0.93 (3H, d, J = 6.3 Hz) attributable to H–30 of an ursane-type framework of **3** (Ibrahim et al. 2012; Khedr et al. 2016). In addition, we noticed signals of an anomeric proton at δ_H 4.27 (1H, d, J = 8.0 Hz, H–1′), three oximethines at δ_H 3.56 (1H, m, H–2′), 3.51 (1H, m, H–3′) and 3.79 (1H, m, H–3′) together with two oxymethylene protons at δ_H 3.50/3.81 (2H, m, H–5′α/*β*) bonded to the carbon at δ_C 66.3 (^{13}C-NMR spectrum), revealing the presence of a xylopyranosyl moiety in **3** (Evina et al. 2017), identified after acid hydrolysis and comparative TLC. The ^{13}C–NMR and HSQC spectra showed the presence of 35 carbons consisting of eight methyls, ten methylenes, ten methines among which, one oxymethine at δ_C 90.7 (C–3), one tri-substituted olefinic double bond at δ_C 129.3 (C–12), one anomeric carbon at δ_C 107.1 (C–1′), and an oxygen-bonded quaternary carbon δ_C 73.7 (C–19). Detailed 1D and 2D NMR analyses of **3**

were similar to those of the known compound 19α-hydroxy-α-amyrin (Akbar and Malik 2002) except for the presence of an additional xylopyranosyl moiety. In the HMBC spectrum (Figure S27), the correlations between H–1′ (δ_H 4.27) and C–3 (δ_C 90.7)/C–5′ (δ_C 66.3) and between H–3 (δ_H 3.12) and C–1′ (δ_C 107.1) indicated that the xylopyranosyl moiety was connected at C–3. The relative orientation of the methyl groups and protons was elucidated based on their NOE correlations, shown in Figure S1. Hence, the absence of NOE between H–18 and H–27, H–5 and H–25, and H–26 and H–27 is diagnostic for their *anti*-orientation. The observed NOEs revealed that H–5, H–9, H–12 and H–27 are α-oriented, whilst H–18, H–25, and H–26 are β-oriented. The assigned relative configuration is in excellent agreement with previous literature reports (Mahato and Kundu 1994; Akbar and Malik 2002; Kim et al. 2012). Hence, the structure of **3** was assigned as 3-*O*-β-D-xylopyranosyl-19α-hydroxy-urs-12-ene and named atheruroside A.

The HR-ESI-MS spectrum of compound **4** exhibited a *quasi*-molecular ion at *m/z* 575.4066 $[M + H]^+$(calcd. for $C_{35}H_{59}O_6^+$: 575.4075), consistent with the molecular formula of $C_{35}H_{58}O_6$. The ^{13}C-NMR data of **4** were in good agreement with those of **3** except for the nature of monosaccharide moiety (identified as xylose in **3**). The presence of an additional downfield shifted oxymethylene at δ_C 74.4 (C–4′) and a remarkable hydroxylated quaternary carbon at δ_C 80.1 (C–3′) in **4**, suggested the xylopyranosyl moiety in **3** was replaced by an apiofuranosyl one (Xu et al. 2010), in **4** (Table S3). This was confirmed by unique ^{1}H–^{1}H-COSY correlation between H–1′/H–2′, and HMBCs from H–1′ (δ_H 4.97) to C–3 (δ_C 89.4)/C–2′ (δ_C 78.1)/C–3′ (δ_C 80.1), from H–4′α/β to C–1′ (δ_C 112.5)/C–3′ (δ_C 80.1)/C–5′ (δ_C 65.5), from H–5′ (δ_H 3.56) to C–3′ (δ_C 80.1)/C–2′ (δ_C 78.1) and from H–3 (3.03) to C–1′ (δ_C 112.5) (Figure S39). Meanwhile, the small coupling constant of H–1′ with H–2′ (J = 2.5 Hz), implied the β-orientation of H-1′ (Silva and Parente 2004). Additionally, The NOE correlation of H–18 and H–20 and H–29, and the absence of NOE between H–18 and H–30 indicate the α-orientation of OH–19 and strengthened the relative configurations of **4**, which are similar to those of **3**. Therefore, compound **4** was elucidated as 3-*O*-β-D-apiofuranosyl-19α-hydroxy-urs-12-ene and named atheruroside B.

The leaves of *T. atherura* exhibited strong antiplasmodial activity against the chloroquine resistant strain Dd2 (IC_{50} 4.39 ± 0.27 µg/ml with a selectivity index > 22.78 against Vero cells) and were promising against the chloroquine sensitive 3D7 strain (IC_{50} 7.54 ± 0.53 µg/mL, with a selectivity index > 13.26 against Vero cells) respectively as shown in Table S4. The *in vitro* antiplasmodial activity was analyzed in accordance with the system of antiplasmodial activity of Rasoanaivo et al. (1992). According to this norm, an extract is regarded to be very active if IC_{50} < 5 µg/mL, moderately active if 5 < IC_{50} < 50 µg/mL, weakly active when 50 µg/mL < IC_{50} < 100 µg/mL and inactive with an IC_{50} > 100 µg/mL. At this stage, the results of the evaluation of the possible risks associated with the application of *T. atherura* extract found in this study indicate that this plant possesses active components capable of inhibiting *P. falciparum in-vitro* with weak cytotoxic effects as regards to its traditional use (Table S4). The antimalarial activity exhibited by the compounds tested (**1**, **4, 5** and **8)** was rather low (64.99 µg/mL to > 100 µg/mL) (Table S4). The most active compound against the chloroquine-resistant Dd2 was atheruramine (**1**), suggesting that alkaloids should be the most active components within the plant, in agreement with moderate antimalarial activities previously reported for some alkaloids (Staerk et al. 2000; Irungu et al. 2014; Puteri et al. 2019). Compounds in the extract might act synergistically hence leading to high antiplasmodial activity of the methanol extract. The results suggest that *T. atherura* could be ranked among true antimalarials, according to a previous report regarding pharmacopeia of the whole genus (He et al. 2002). This is the first

ever report on potential *in-vitro* antimalarial activity of *T. atherura*. Additional survey should be carried on *T. atherura* aiming to develop at least one antimalarial drug.

3. Experimental (in supplementary data)

4. Conclusions

The phytochemical investigation of *T. atherura* resulted in the discovery of twelve compounds. Among them, atheruramine (**1**), tricalydioloside (**2**) and atherurosides A and B (**3** and **4**) are described for the first time. In addition, compounds **1**, **4**; **5** and **8** displayed slight *in vitro* antiplasmodial activitiy against Dd2 strains of *P. falciparum* with IC_{50} values ranging from 64.99 to 92.29 µg/mL. Notably, compound **1** showed the strongest antiplasmodial activity among the isolates. However, the leaves extract of *T. atherura* possesses high antiplasmodial activities against *P. falciparum* with relatively low cytotoxicity. This study suggested that alkaloids and triterpenes might be the major active components contributed to the antiplasmodial activity of *T. atherura.*

Acknowledgments

The authors thank Mr. Victor Nana (National Herbarium of Cameroon) for his assistance in the collection and identification of the plant material. The authors also acknowledge the laboratory for Phytobiochemistry and Medicinal Plant Studies, Antimicrobial and Biocontrol Agents Unit, at the Department of biochemistry of the University of Yaounde I in Cameroon for antiparasite and cytotoxic activities.

Disclosure statement

The authors report no declarations of interest.

Funding

The authors acknowledge The World Academy of Science (TWAS) and the International Center for Chemical and Biological Sciences (ICCBS), University of Karachi, Karachi, Pakistan for the Postgraduate Fellowship number: 3240311210 granted to Djikam Sime Gwladys.

References

Agata I, Hatano T, Nishibe S, Okuda T. 1988. Rabdosiin: a new rosmarinic acid dimer with a lignin skeleton from Rabosia japonica. Chem Pharm Bull. 36(8):3223–3225.

Akbar E, Malik A. 2002. Antimicrobial triterpenes from Debregeasia salicifolia. Nat Prod Lett. 16(5):339–344.

Akhtar N, Malik A, Ali SN, Kazmi SU. 1994. Rubrinol, a new antibacterial triterpenoid from Plumeria rubra. Fitoterapia. 65:162–166.

Awouafack MD, Tane P, Morita H. 2018. Tricalycoside, a new cerebroside from Tricalysia coriacea (Rubiaceae). Chem Biodiv. 15:1–6.

Barreiro EJ. 1990. Produtos naturais bioativos de origem vegetal e o desenvolvimento de fármacos. Quím Nova. 13:29–39.

Bartlett MF, Sklar R, Taylor WI, Schlittler E, Amai RLS, Beak P, Bringi NV, Wenkert E. 1962. Rauwolfia alkaloids. XXXVIII.1 Stereospecific degradations leading to the absolute configurations and structures of ajmaline, sarpagine and corynantheidine. J Am Chem Soc. 84(4):622–630.

Battersby AR, Yeowell DA. 1964. Alkaloids of calabash-curare and Strychnos species. Part III. Structure and absolute stereochemistry of macusine-A, macusine-B, and macusine-C. J Chem Soc. 0:4419–4427.

Bitombo AN, Zintchem AA, Atchadé AT, Ndedi EDFM, Khan A, Bikobo DSN, Pegnyemb DE, Bochet CG. 2022. Antimicrobial and cytotoxic activities of indole alkaloids and other constituents from the stem barks of Rauvolfia caffra Sond (Apocynaceae), Nat Prod Res. 36(6): 1467–1475.

Bouquet A. 1972. Plantes médicinales du Congo-Brazzaville. Uvariopsis, Pauridiantha, Diospyros. O.R.S.T.O.M, Paris, p 113. (Travaux et Documents de l'ORSTOM; 13). Th.: Botanique: Paris.

Bridson DM, Verdcourt B. 2003. Rubiaceae. Flora Zambesiaca 5(3):379–720. Royal Botanic Gardens, Kew, UK.

Brown RT, Charalambides AA. 1974. 5α-Carboxytetrahydroalstonine. Tetrahedron Lett. 17:1649–1652.

Bruschi P, Morganti M, Mancini M, Signorini MA. 2011. Traditional healers and laypeople: a qualitative and quantitative approach to local knowledge on medicinal plants in Muda (Mozambique). J Ethnopharmacol. 138(2):543–563.

De Silva KTD, King D, Smith GN. 1971. J Chem Soc., Chem Commun. 16:908–909.

Elliot S. 1986. Pharmacy needs tropical forests. Manuf Chem. 57:31–34.

Evina JN, Bikobo DSN, Zintchem AA, Nyemeck NM, IINdedi EDFM, Diboué PHB, Nyegue MA, Atchadé AT, Pegnyemb DE, Koert U, et al. 2017. In vitro antitubercular activity of extract and constituents from the stem bark of Disthemonanthus benthamianus. Braz J Pharmacol. 27(6):739–743.

Farias FM. 2006. [*Psychotria myriantha* müll arg. (Rubiaceae): Caracterização dos alcalóides e avaliação das atividades antiquimiotáxica e sobre o sistema nervoso central]. [Ph.D. Thesis]. Porto Alegre, RS, Brazil: Universidade Federal do Rio Grande do Sul.

Gołembiewska E, Skalicka-Wózniak K, Głowniak K. 2013. Methods for the isolation and identification of triterpenes and sterols in medicinal plants. Curr. Issues Pharm Med Sci. 26:26–32.

Greve HL, Kaiser M, Brun R, Schmidt TJ. 2017. Terpenoids from Oleo-Gum-Resin of Boswellia serrata and their antiplasmodial effects in vitro. Planta Med. 83(14-15):1214–1226.

He DH, Otsuka H, Hirata E, Shinzato T, Bando M, Takeda Y. 2002. Tricalysiosides A − G: rearranged ent-kauranoid glycosides from the leaves of Tricalysia dubia. J Nat Prod. 65(5):685–688.

Ibrahim SRM, Mohamed GA, Shaala LA, Banuls LMY, Van Goietsenoven G, Kiss R, Youssef DTA. 2012. New ursane-type triterpenes from the root bark of Calotropis procera. Phytochem Lett. 5(3):490–495.

Irungu BN, Orwa JA, Gruhonjic A, Fitzpatrick PA, Landberg G, Kimani F, Midiwo J, Erdélyi M, Yenesew A. 2014. Constituents of the roots and leaves of Ekebergia capensis and their potential antiplasmodial and cytotoxic activities. Molecules. 19(9):14235–14246.

Khedr AIM, Ibrahim SRM, Mohamed GA, Ahmed HEA, Ahmad AS, Ramadan MA, Abd El-Baky AE, Yamada K, Ross SA. 2016. New ursane triterpenoids from Ficus pandurata and their binding affinity for human cannabinoid and opioid receptors. Arch Pharm Res. 39(7):897–911.

Kiang AK, Loh SK, Demanczyk M, Gemenden CW, Papariello GJ, Taylor WI. 1966. The structures of peraksine (RP-5) and RP-7 constituents of the leaves and stems of Rauwolfia perakensis. Tetrahedron. 22(10):3293–3300.

Kim KH, Choi SU, Lee KR. 2012. Cytotoxic triterpenoids from Berberis koreana. Planta Med. 78(1):86–89.

Laurens MB. 2020. RTS,S/AS01 vaccine (MosquirixTM): an overview. Hum Vaccines Immunother. 16(3):480–489.

Li LQ, Li J, Huang Y, Wu Q, Deng SP, Su XJ, Yang RY, Huang JG, Chen ZZ, Li S. 2012b. Lignans from the heartwood of Streblus asper and their inhibiting activities to hepatitis B virus. Fitoterapia. 83(2):303–309.

Lim QY, Tan SP, Tan HY, Liew WK, Lau YL, Nafiah MA. 2021. Compounds Isolated from Bark of Phyllanthus acidus (L.) Skeels. Malaysian J Chem. 23:165–172.

Li J, Tang MJ, Wu Q, Chen H, Niu XT, Guan XL, Li J, Deng SP, Su XJ, Yang RY. 2012a. Water-soluble Constituents of the Heartwood of Streblus asper. Nat Prod Com. 7:497–500.

Mabberley DJ. 1990. The plant-book: a portable dictionary of the vascular plants utilizing Kubitzki's the families and genera of vascular plants.

Mahato SB, Kundu AP. 1994. 13C NMR spectra of pentacyclic triterpenoids – acompilation and some salient features. Phytochemistry. 37(6):1517–1575.

Mongrand S, Badoc A, Patouille B, Lacomblez C, Chavent M, Bessoule JJ. 2005. Chemotaxonomy of the Rubiaceae family based on leaf fatty acid composition. Phytochemistry. 66(5):549–559.

Moshi MJ, Otieno DF, Weisheit A. 2012. Ethnomedicine of the Kagera Region, North Western Tanzania. Part 3: plants used in traditional medicine in Kikuku Village, Muleba District. J Ethnobiol Ethnomed. 8(2012):14.

Nishimura K, Hitotsuyanagi Y, Sugeta N, Fukaya H, Aoyagi Y, Hasuda T, Kinoshita T, Takeya K. 2007. Tricalysiamides A − D, Diterpenoid Alkaloids from Tricalysia dubia. J Nat Prod. 70(5):758–762.

Nishimura K, Hitotsuyanagi Y, Sugeta N, Sakakura KI, Fujita K, Fukaya H, Aoyagi Y, Hasuda T, Kinoshita T, He DH, et al. 2006. Tricalysiolides A-F, new rearranged ent-kaurane diterpenes from Tricalysia dubia. Tetrahedron. 62(7):1512–1519.

Nogueira PCN, Araújo RM, Viana GSB, de Araújo DP, Braz Filho R, Silveira ER. 2014. Plumeran Alkaloids and Glycosides from the Seeds of Aspidosperma pyrifolium Mart. J Braz Chem Soc. 25:2108–2120.

Parmar VS, Jain SC, Gupta S, Talwar S, Rajwanshi VK, Kumar R, Azim A, Malhotra S, Kumar N, Jain R, et al. 1998. Polyphenols and alkaloids from Piper species. Phytochemistry. 49(4):1069–1078.

Pereira CG, Meireles MAA. 2010. Supercritical fluid extraction of bioactive compounds: fundamentals, applications and economic perspectives. Food Bioprocess Technol. 3(3):340–372.

Puteri A, Nugroho AE, Hirasawa Y, Kaneda T, Tougan T, Horii T, Morita H. 2019. Two new sarpagine-type indole alkaloids and antimalarial activity of 16-demethoxycarbonyl voacamine from Tabernaemontana macrocarpa Jack. J Nat Med. 73(4):820–825.

Rasoanaivo A, Ravi P, Petitjean S, Ratsimamanga-Urverg A, Rakoto R. 1992. Medicinal plants used to treat malaria in Madagascar. J Ethnopharmacol. 37(2):117–127.

Robbrecht E. 1987. The African genus Tricalysia A. Rich. (Rubiaceae): 4. A revision of the species of sectio Tricalysia. Bull Nat Plantentuin Belg. 57(1/2):39–208.

Silva BP, Parente JP. 2004. New Steroidal Saponins from Rhizomes of Costus spiralis. Z Naturforsch C J Biosci. 59(1-2):81–85.

Sonké B, CHeek M, Nambou DM, Robbrecht E. 2002. A new species of Tricalysia A. Rich. (Rubiaceae) from western Cameroon. Kew Bull. 57(3):681–686.

Staerk D, Lemmich E, Christensen J, Kharazmi A, Olsen CE, Jaroszewski JW. 2000. Leishmanicidal, antiplasmodial and cytotoxic activity of indole alkaloids from Corynanthe pachyceras. Planta Med. 66(6):531–536.

World Health Organization 2004. World health report 2003. Available at http://www.who.int/whr/2003/en.

World Health Organization 2020. World Malaria Report. The “World malaria report 2020” at a glance. WHO: Geneva, Switzerland. Available from http://www.who.int/teams/global-malaria-programme/report/world-malaria-report-2020. Accessed on 3rd March, 2021.

World Health Organization 2021. WHO recommends groundbreaking malaria vaccine for children at risk. Available from https://who.int/news/item/06-10-2021-who-recommends-groundbreaking-malaria-vaccine-for-children-at-risk. Accessed on 31st October, 2021.

Xu WH, Jacob MR, Agarwal AK, Clark AM, Liang ZS, Li XC. 2010. Ent-Kaurane Glycosides from Tricalysia okelensis. Chem Pharm Bull (Tokyo). 58(2):261–264.